JOURNAL OF MATERIALS SCIENCE 28 (1993) 6274–6278

Electrophoretic deposition and its use to synthesize ZrO_2/Al_2O_3 micro-laminate ceramic/ceramic composites

P. S. NICHOLSON, P. SARKAR, X. HAUNG
Ceramic Engineering Research Group, Department of Materials Science and Engineering, McMaster University, Hamilton, Ontario, Canada L8S 4L7

Electrophoretic deposition has been employed to synthesize yttria-stabilized zirconia (YSZ)/alumina, laminar microcomposites with a total of 80 layers, > 2 mm. 10 wt% solids, ethanol suspensions of YSZ or Al_2O_3 powders were deposited layer by layer. The deposited samples had a green density, ~ 60% theoretical. The deposition process was characterized by the rate-of-deposition as a function of voltage and the microstructure of the sintered, theoretically dense samples was characterized by optical and electron microscopy. Microindentation was used to explore the mechanical properties of the laminates.

1. Introduction

Laminar ceramic composites are at present synthesized by tape casting [1, 2], slip casting [3], centrifugal casting [4] and dough rolling [5]. The room-temperature strength [2] and fracture toughness [4, 5] are significantly improved compared to ceramic monoliths. One important factor controlling the performance of a ceramic laminate is the lamellar thickness as it controls the extent of crack propagation before interception of an interface. Boch *et al.* [1, 2] tape cast laminar composites of alternate layers of Al_2O_3 and Al_2O_3/ZrO_2 (up to 10 wt % ZrO_2) with a minimum layer thickness of 150 μm. Requena *et al.* [3] synthesized Al_2O_3 and Al_2O_3/ZrO_2 (4 wt % ZrO_2) laminates by slip casting to a minimum layer thickness, ~ 100 μm. Marshall *et al.* [4] used centrifugal casting to fabricate cerium-stabilized ZrO_2/(50 wt %) dispersed Al_2O_3 laminates. The minimum layer thickness quoted was 10 μm. Zirconia is added to the alumina layers to avoid cracking during processing. This cracking problem can be eliminated by reducing the layer thickness.

The present paper describes the synthesis of laminar microcomposites with minimum layer thickness as low as ~ 2 μm and submicrometre interfacial smoothness, by electrophoretic deposition (EPD). Complex shapes can be fabricated by this technique in a single step with no organic binders, lubricants or plasticizers.

2. Electrophoretic deposition

Electrophoretic deposition (EPD) is the process whereby powder particles are deposited from a suspension on to a shaped electrode of opposite charge, on application of a d.c. electrical field. The rate of deposition is controllable via applied potential and can be very fast.

EPD is two processes: electrophoresis, the motion of particles in a stable suspension under the influence of an electrical potential gradient; and deposition, the coagulation of a dense layer of particles on the electrode. Stability is introduced electrostatically and/or physically ("steric hinderance"). The latter involves adsorption of molecules with polymeric tails that physically maintain the interparticle distance.

Dealing first with electrostatic stability, when a particle is submerged in a liquid, the electrochemical nature of its surface changes. Ions leave or are adsorbed and the particle assumes a surface charge. This is balanced by ions or polar molecules residing in the liquid near the surface. Immediately adjacent to the surface this "double-layer" of charge is dense. Further out it is diffuse.

When the particle moves, some of the ions in the diffuse region "shear-off" and the potential developed between the particle surface and the shear layer boundary is termed the zeta-potential, ζ. Particles repel and the higher the ζ, the more stable is the suspension against coagulation (coagulation is due to the London–van der Waals (LVDW) attractive forces which operate on very close particle approach). The sign of the charge on the particle is the same as its surface for the latter is now incompletely balanced by the double layer.

To appreciate the mechanism of EPD for laminar ceramic synthesis, the process will be compared with that of slip casting (pressure casting, centrifugal casting). In both cases a dense deposit forms so the charges that served to maintain the particles apart must be reduced to a level conducive with coagulation. In slip casting, the deposit forms by liquid removal. The particles cannot enter the mould capillaries so build up on the surface. Ions of *both* signs will be drawn with the particles as the liquid moves and the liquid motion through the deposited stationary particles at a higher

0022–2461

velocity will thin the diffuse double layers so ζ drops and LVDW forces induce coagulation. It is interesting to note that, as the particle and its double layer move with the liquid, the symmetry of the double layer around the particle will be undistorted.

In EPD the particles move in a stationary liquid and ions of both signs do not move with the particles – just those of the *same* sign. The particles coagulate so their double layers must be thinned and two mechanisms by which this might occur will now be described. As the particles move in a stationary liquid, their diffuse double layers will distort, tailing out behind the particles. This distortion is further promoted by the ions in the double layer being attracted to the *other* electrode in the system. This distortion results in diffuse double-layer thinning ahead and to the equator of the electrophoresing particles, reducing ζ there.

The second possible ζ reduction mechanism is the result of the free ions of the *same* sign as the particles that move with the particles. Some of these discharge at the electrode or are involved in electrode reactions to give the current but a number will be available to react with the ions of opposite sign in the diffuse double layers to reform the electrolyte molecules. This reformation will be promoted by the increased local ionic concentration changing the original dissociation equilibrium; i.e. the reaction

$$\text{salt/acid/alkali} \rightleftharpoons \text{cations} + \text{anions} \qquad (1)$$

is driven to the left. This process will also thin the diffuse double layer and allow sufficiently close particle approach for LVDW forces to induce coagulation. This mechanism will be enhanced by the distortion of the diffuse double layer. The ions in the double layer "tail" are weakly held therein by the particle, being further from its centre-of-charge, and so will react with the counter-ions more readily. This will also be true for stationary particles in the surface of the deposit, because the other electrode will distort their combined diffuse double layers, rendering them vulnerable to counter-ion reaction and destruction.

The neutral molecules of electrolyte that reform local to the electrode will diffuse down their concentration gradient with the bulk suspension to re-dissociate in the more rarified ionic atmosphere therein, thus allowing those ions that used to be in the diffuse double layers to discharge at the other electrode. Thus ions in the particle diffuse layers are indirectly involved in the current passage.

It is also possible that the ions in the diffuse double layer react with other neutral molecules in the system around the particles and the electrons supplied or accepted by the electrode, to discharge the double-layer ions.

The motion of particles in a stationary liquid raises interesting ramifications for the development of microstructural texture in electrophoretically deposited ceramics. Whereas anisotropic, "platey" particles will tend to lie parallel to a slip-casting mould wall (like playing cards on a suction fan), travel through a stationary liquid during electrophoresis will align such particles edge-on and, if the charges are associated with these edges as they are, for instance, with Na–β''-Al_2O_3 [6], this orientation could survive in the deposit, i.e. 90° to the slip-cast orientation. There is no direct evidence of such microstructural morphology in Na–β''-Al_2O_3, but electrophoretically deposited tubes of the material are more conductive than their isopressed counterparts ($\sim 3\ \Omega$cm resistance at 350 °C compared to 4–5 Ωcm).

The role of charges in the EPD process requires the dielectric constant, e, of the suspension be maximum. The ideal would be water ($e = 80$) but electrolysis occurs, so organic liquids (methanol (33), ethanol (24), propanol (18) and acetone (21)) are used. The present investigations utilized ethanol and the natural ions in the Al_2O_3 and ZrO_2 powders.

Steric-hinderance induced stability may play a role in the present systems, particularly Al_2O_3. Brown and Salt [7] suggested $Al(OH)_3$ of polymeric structure forms on aluminium particles in ethyl alcohol when $AlCl_3$ is added to the system. These "coatings" of $Al(OH)_3$ maintain the particles apart, rendering the suspension stable. It is reported [8] that commercial ZrO_2 powders contain Cl^- and this may permeate the system and induce steric-hinderance stability.

The mode of transformation from deflocculated to coagulated particles is an advantage of the EPD process. The solids concentration in the suspension is low (< 3 vol %) so there is minimal particle interaction. The deposition rate is comparable with slip and pressure casting because it is controlled by the applied voltage. Adjustment of the latter parameter can also control the deposition rate to be constant, a degree of control not available in slip casting; green densities of 60% theoretical can be achieved. At such low concentrations there are no thixotropic tendencies and, as the deflocculated–coagulated transformation is induced electrically, the process is more controllable. The elimination of soft agglomerates by mixing and hard agglomerates and inclusions by settling, is also much more effective in the low volume per cent solid suspensions of EPD.

As the greenware contains no organics, no burn-out procedures are required and a deposit can be formed on the outside and/or the inside of the electrode. Inside deposition is useful for closed-end tubes, because shrinkage is unrestricted by the rigid electrode. Electrode removal from the greenware is facilitated by polishing the former or employing a shape of conducting paper or plastic.

EPD techniques have been used to deposit inorganic coatings on fine wires for valve filaments and cathodes and wax on to metals [9]. In 1969, Andrews *et al.* [10] fabricated monolithic alumina bodies by EPD and at present the technique is used to synthesize β-and β''-alumina ceramics [11–15]. Rao *et al.* [16] used the technique to fabricate magnesia ceramics, and high T_c superconductors thick films have been grown by EPD [17–23]. To utilize the anisotropic transport properties of the high T_c superconductors, Hein *et al.* [20] produced textured $YBa_2Cu_3O_x$ films electrophoretically with a magnetic field applied perpendicular to the deposition surface. Sarkar and Nicholson [22, 23] synthesized textured thick films of

$BiSrCaCuO$ and $YBa_2Cu_3O_x$ superconductors by EPD using high aspect ratio powder.

3. Microlaminate fabrication

Two suspensions were formulated; 10 wt % Al_2O_3 (Sumitomo, Tokyo AKP-50) and 10 wt % 3% yttria-stabilized zirconia (YSZ) (Tosoh, Tokyo, TZ-3Y) both in ethanol. Each was vibromilled for 20 h. Layers were deposited sequentially on a graphite electrode (cathode). The separation between the two EPD electrodes was 1 cm and a constant voltage (0–600 V) power source was used for the deposition. After deposition, samples were dried and separated from the electrode. The green density of the deposit was $\sim$ 60% theoretical. The composites were sintered at 1550 °C for 6 h with a heating and cooling rate of 300 °C h^{-1}.

4. Results and discussion

Fig. 1 is a plot of the deposit thickness versus time for two constant voltages (75 and 125 V cm^{-1}). The thickness was calculated from the deposit weight using the theoretical density of the materials. The results show that, for any given time and voltage, the thickness of the YSZ layer is less than that of Al_2O_3. It also shows the rate of deposition decreases with time. The deposition current density also decreases with time (Fig. 2) resulting in a decreased rate of deposition. There are two reasons for the decrease of current density; electrode polarization and/or the formation of an insulating deposit layer (Al_2O_3 or YSZ). The voltage drop due to electrode polarization should reach a steady value very fast but resistance due to the build up of an insulating deposit will increase continuously as deposition progresses. The deposition voltage had to be increased as deposition progressed, thus the resistance of the deposit is the major source of voltage drop.

Fig. 3a is a low-magnification scanning electron micrograph of an 80 layer microlaminate of total thickness $\sim$ 1.5 mm. Fig. 3b is a higher magnification of (a) showing the thickness of the YSZ layer is $\sim$ 2 μm i.e. about three grain thicknesses. The interface uniformity is in the submicrometre range and is well bonded. The thickness of the Al_2O_3 layer in these micrographs is $\sim$ 12 μm; the overall volume percentage YSZ is $\sim$ 15% and the composite has a porosity < 0.5 vol %. The Al_2O_3 grain size is large and steps are presently being taken to reduce it by grain-growth inhibitors and decreasing temperature. Fig. 4 displays the controllability of the EPD process; the YSZ layers have uniform thickness $\sim$ 7 to $\sim$ 18 μm.

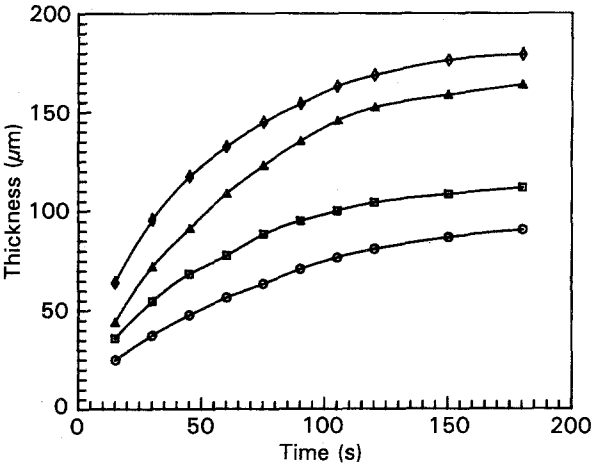

Figure 1 Deposition thickness at (△, ○) 75 and (◇, □) 125 V cm^{-1} of (◇, △) Al_2O_3 and (□, ○) YSZ as a function of deposition time.

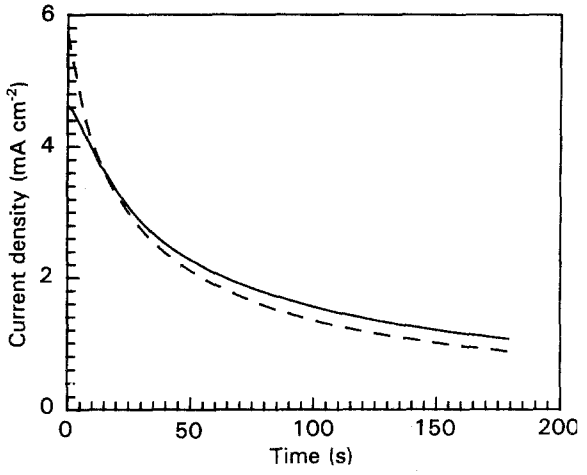

Figure 2 Deposition current density for (———) Al_2O_3 and (---) YSZ at 125 V cm^{-1} as a function of deposition time.

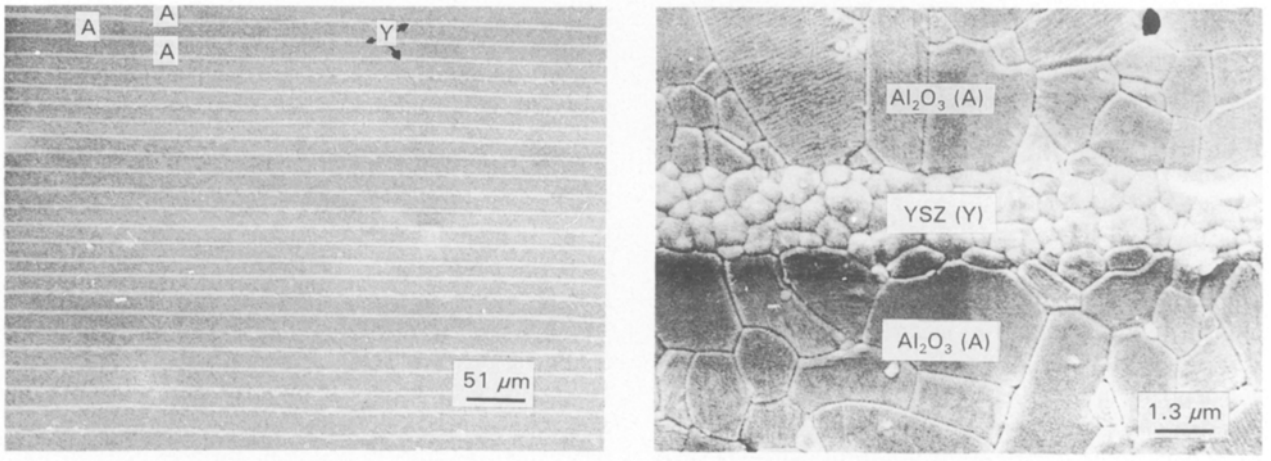

Figure 3 Scanning electron micrographs of Al_2O_3/YSZ microlaminate (a) low magnification, and (b) high magnification.

Fig. 5a is a fractograph of a laminate broken by bending normal to the laminate surface at room temperature. The dominant fracture mode was intergranular in the Al_2O_3 layers, intergranular in the YSZ layers. Subsurface microcracks are visible in the YSZ layers indicating some tetragonal– monoclinic phase transformation was triggered during the fracture. The lamellae exhibit fracture characteristics similar to those of bulk Al_2O_3 and YSZ. The interface between Al_2O_3 and YSZ is well defined and dense. No debonding occurred during fracture. A few YSZ particles are located in the Al_2O_3 layer close to the interface and did not limit grain growth in the bulk of the Al_2O_3 layers.

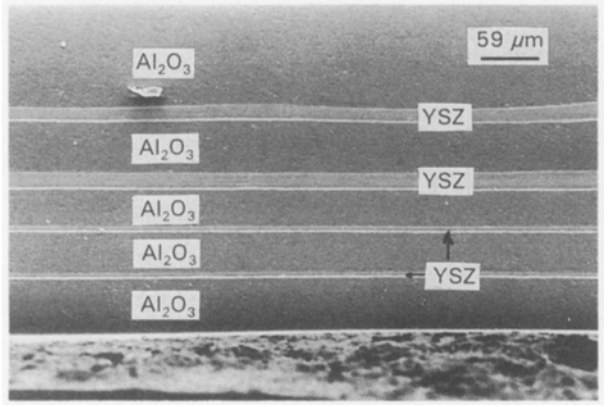

Figure 4 A scanning electron micrograph of a variable thickness laminate.

Fig. 5b is a room-temperature Vickers indentation on a polished cross-section of the laminate. The indent was made on a polished surface at $\sim 45°$ to the YSZ layers with a load of 5 Kgf. During polishing, some Al_2O_3 grains pulled out, leaving white features on the micrograph. The indent corners are located in the Al_2O_3 layers and the cracks would normally extend along the directions of the indent diagonals in an Al_2O_3 monolith. The YSZ layers divert the cracks from their normal paths towards the interlaminar interfaces. This deflection is more obvious when the indent corners are close to an Al_2O_3/YSZ interface. There was also some microcrack damage near and across the interface. These observations suggest crack deflection is an operating toughening mechanism in these electrophoretically deposited Al_2O_3/YSZ microlaminates. The increased anisotropy of the Knoop indent geometry supports this mechanism (Fig. 6a and b). An indent with the long axis perpendicular to the plane of the laminations induced minimal tip-cracking (Fig. 6a). Substantial cracking was induced, on the other hand, when the axis was parallel to the laminations (Fig. 6b; the reader should ignore the crack in the upper right quadrant of this micrograph. It initiated from the tip of a subsequent indent, curling towards the indent in question).

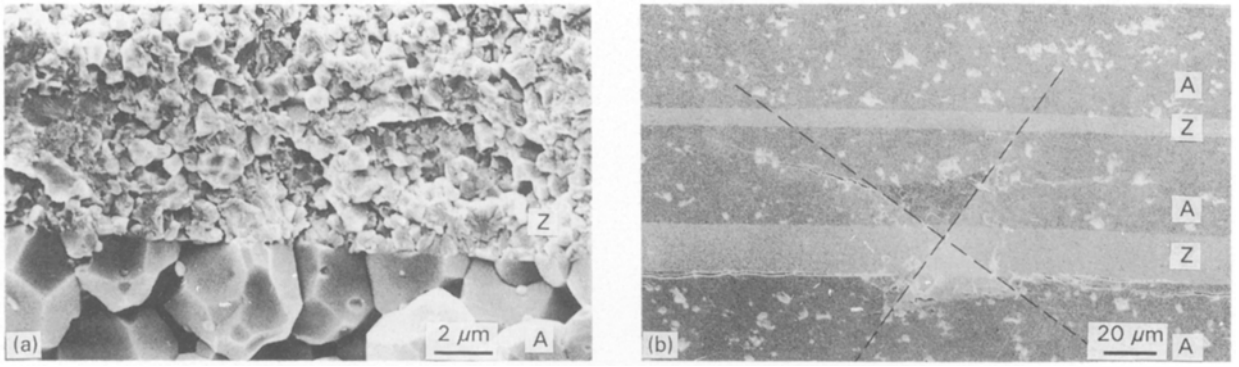

Figure 5 (a) Room-temperature fracture surface of an Al_2O_3/YSZ laminate. A = Al_2O_3, Z = ZrO_2. (b) Indentation fracture of an Al_2O_3/YSZ laminate. A = Al_2O_3, Z = ZrO_2. (---) The ideal crack growth direction.

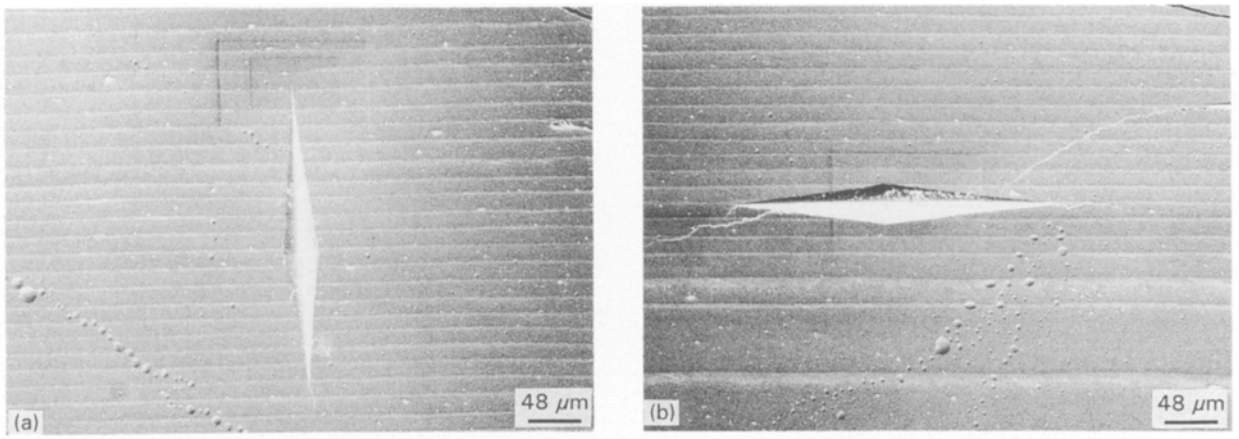

Figure 6 (a) Knoop indent perpendicular to lamination of Al_2O_3/YSZ laminate. (b) Knoop indent parallel to laminations of Al_2O_3/YSZ laminate (ignore crack at top right quadrant – from a subsequent indent).

5. Conclusion

Although electrophoretic deposition has been used for many years to fabricate monolithic ceramics, this paper reports its first use to synthesize ceramic/ceramic laminates.

The EPD process is described via comparison with the more conventional casting techniques and its advantages over the latter are discussed. It is demonstrated that electrophoretic deposition is an effective technique to synthesize laminar Al_2O_3/YSZ ceramic microcomposites. The minimum layer thicknesses achievable are in the few micrometres range with interfacial perfection in the submicrometre range.

References

1. P. BOCH, T. CHARTIER and M. HUTTEPAIN, *J. Am. Ceram. Soc.* **69** (1986) C 191.
2. T. CHARTIFUL, J. L. BESSON and P. BOCH, in "Advances in Ceramics" Vol. b, "Science and Technology of Zirconia III," edited by Somiya, N. Yamamoto and H. Yanagida (The American Ceramic Society, 1988) p. 1131.
3. J. REQUENA, R. MORENO and J. S. MOYA, *J. Am. Ceram. Soc.* **72** (1989) 1511.
4. D. B. MARSHALL, J. J. RATTO and F. F. LANGE, *ibid.* **74** (1991) 2979.
5. W. J. CLEGG, K. KENDALL, N. McNALFORD, T. W. BOTTON and J. D. BIRCHALL, *Nature* **347** (1990) 455.
6. S. N. HEAVENS, in "Novel Ceramic Fabrication Processes and Applications", edited by R. W. Davidge (British Ceramic Proceedings, London, UK, 1986) p. 119.
7. D. R. BROWN and F. W. SALT, *J. Appl. Chem.* **15** (1965) 40.
8. H. TAKEBE, N. YOSHIHAMA and K. MORINAGE, *J. Am. Ceram. Soc. Jpn Int. Ed.* **98** (1990) 140.
9. J. B. BIRKS, "Progress in Dielectrics", Vol. I, edited by J. B. Birks and J. H. Schulman (Heywood, London, 1959).
10. J. M. ANDREWS, A. H. COLLINS, D. C. CORNISH and J. DRACASS, *Proc. Br. Ceram. Soc.* **211** (1969) 211.
11. J. H. KENNEDY and A. FOISSY, *J. Electrochem. Soc.* **122** (1975) 482.
12. R. W. POWERS, *ibid.* **122** (1975) 490.
13. A. A. FOISSY and G. ROBERT, *Am. Ceram. Soc. Bull.* **61** (1982) 251.
14. R. W. POWERS, *ibid.* **65** (1986) 1270.
15. *Idem, ibid.* **65** (1986) 1277.
16. D. U. KRISHNA RAO and E. C. SUBBARAO, *ibid.* **58** (1979) 467.
17. C. T. CHU and B. DUNN, *Appl. Phys. Lett.* **55** (1989) 492.
18. H. S. MAITI, S. DATTA and R. N. BASU, *J. Am. Ceram. Soc.* **72** (1989) 1733.
19. H. S. MAITI, R. N. BASU and S. DATTA, *Phase Transitions* **19** (1989) 139.
20. M. HEIN, G. MILLER, H. PIEL and L. PONTO, M. BECKS, U. KLEIN and M. PEINIGER, *J. Appl. Phys.* **66** (1989) 5940.
21. H. NOJIMA, H. SHINTAKU, M. NAGATA and M. KOBA, *Jpn J. Appl. Phys.* **30** (1991) L1166.
22. P. SARKAR and P. S. NICHOLSON, *J. Appl. Phys.* **69** (1991) 1775.
23. *Idem, J. Appl. Phys. Lett.* **61** (1992) 492.

Received 30 July 1992
and accepted 10 February 1993